Single-cell Transcriptome Analysis Indicates New Potential Regulation Mechanism of ACE2 and NPs signaling among heart failure patients infected with SARS-CoV-2

Dachun Xu[1]*, Mengqiu Ma[1]*, Yanhua Xu[1]*, Yang Su[1]*, Sang-Bing Ong[2], Xingdong Hu[3], Min Chai[4], Maojun Zhao[5], Hong Li[6], Xiaojiang Xu[7 #]

[1]Department of Cardiology, Shanghai Tenth People's Hospital, Tongji University School of Medicine, 1239 Siping Road, Shanghai, 200072, China. [2]Department of Medicine and Therapeutics, Chinese University of Hong Kong, Hongkong, China. [3]Department of Critical Care Medicine, The third people's Hospital of Guizhou Province, Guiyang, China. [4]Department of Critical Care Medicine, Ezhou Central Hospital, Ezhou, China. [5]Emergency department, The First People Hospital's of Guiyang, Guiyang, Guizhou, China. [6] IID, NIEHS, National Institutes of Health, Research Triangle Park, NC, 27709, USA. [7]Integrative Bioinformatics, ESCBL, NIEHS, National Institutes of Health, Research Triangle Park, NC, 27709, USA

* Dachun Xu, Mengqiu Ma, Yanhua Xu and Yang Su contributed equally to this work.

Correspondence**:** Xiaojiang Xu, Ph.D. Email: xiaojiang.xu@nih.gov.

Abstract

The coronavirus disease 2019 (COVID-19) has resulted in high morbidity and mortality worldwide since December 2019. Recent studies showed that patients with previous heart disease, especially heart failure (HF), whose plasma Natriuretic Peptides (NPs) concentrations are higher, were more susceptible to SARS-CoV-2 infection. In this study, we retrospectively analyzed single-center case series of 91 patients with COVID-19 in China. 46 (50.5%) patients exhibited cardiac dysfunction as indicated by elevated Natriuretic Peptides B (BNP) levels. Moreover, the results indicate that patients with cardiac dysfunction had higher mortality than those without cardiac dysfunction. Nonetheless, it remains unclear as to how the virus infects the heart, especially in HF patients and why a higher level of BNP in the heart dampen inflammation. Angiotensin-converting enzyme 2 (ACE2), the critical host cellular receptor of SARS-CoV-2, expresses in different organs. Still, its cellular distribution in the human heart, especially in patients with HF remains unclear. Thus, we investigated ACE2 gene expression pattern in single-cell RNA sequence (scRNA-seq) data of hearts from normal adults versus patients with HF. Our results indicate that ACE2 is predominantly enriched in cardiomyocytes (CMs), endothelial cells, fibroblasts and smooth muscle cells in normal heart. Not only ACE2+ CMs, but also expression of ACE2 are significantly boosted in CMs of patients with HF. Also, genes related to virus entry, virus replication and suppression of IFN-γ signaling besides ACE2 were up-regulated in HF patient, mainly in CMs, indicating the higher susceptibility to SARS-CoV-2 infection. Interestingly, NPs are significantly up-regulated in ACE2-postive (ACE2+) ventricular myocytes and share the upstream transcription factor. ACE2 and NPs can form a negative feedback loop with protective effects. But it maybe turns into a positive feedback loop by virus and ineffective NPs, which lead to severe prognosis. In summary, the increased

expression of ACE2, NPs during HF predisposes to SARS-CoV-2 infection. Modulating the levels of ACE2, NPs therefore may potentially be a novel therapeutic target to prevent the SARS-CoV-2 infection.

Running title: scRNA-seq and ACE2 and NPs signaling in COVID-19 with heart failure

Keywords: COVID-19, SARS-CoV-2, Heart failure, Cardiac dysfunction, Angiotensin converting enzyme 2, Single-cell sequence

Introduction

A novel disease termed Coronavirus Disease 2019 (COVID-19) caused by severe acute respiratory syndrome, coronavirus 2(SARS-CoV-2) broke out in December 2019[1]. The virus has spread worldwide and classified as a pandemic in 2020. As of April 2020, more than 30 million cases of COVID-19 and more than 200,000 deaths have been reported worldwide[2]. Besides respiratory illness, the viral infection causes a series of symptoms related to myocardial injury, including cardiac dysfunction[1, 3, 4]. Recent clinical studies have found that the elderly and individuals with underlying comorbidities, including cardiovascular diseases such as hypertension (HTN) and coronary heart disease (CAD) are more susceptible to SARS-CoV-2 with worse prognosis[5, 6]. Cardiac injury has also been found to be a common condition among hospitalized patients with COVID-19 and is associated with a higher risk of in-hospital mortality[5].

Single-cell RNA sequencing has shown that the SARS-CoV-2 entry receptor, angiotensin-converting enzyme 2 (ACE2) is highly expressed in the nasal, kidney, endothelium, testis, and heart[7-12]. Zou *et al.* reported that cardiomyocytes (CMs) contained ACE2 positive cells, thus

raising the possibility of the myocardium being infected with SARS-CoV-2[9]. ACE2 functions to convert angiotensin II (Ang II) into angiotensin1-7 (Ang1-7) thus preserving ejection fraction in patients with HF[13]. As such, patients with underlying cardiovascular disorders such as HF are more susceptible to be infected by the virus and their mortality rates are higher than compared to normal patients resulting from increased ACE2[14]. Nonetheless, at the single cell level, nothing much is known about the underlying mechanism as to why the failing heart is more vulnerable to the virus compared with a normal heart.

Our present study retrospectively analyzed a single-center case series in Ezhou, China. The results show that cardiac dysfunction（BNP≥100 pg/mL）in patients infected with SARS-CoV-2 is associated with higher mortality. We then applied single-cell RNA sequencing (scRNA-seq) to hearts from the normal adults versus patients with failing heart to elucidate the potential mechanisms of acute myocardial injury caused by SARS-CoV-2 infection. ACE2 transcript was detected in all types of cells in heart, including cardiomyocytes (CMs), endothelial, fibroblasts and smooth muscle cells and immune cells. A type of abnormal CMs (CM4) was identified specifically in HF patients. Genes related to virus entry, virus replication and suppression of IFN-γ signaling besides ACE2 were up-regulated in HF patient. Interestingly, ACE2-postive (ACE2+) ventricular myocytes expressed high NPs. We demonstrated that the increased expression of ACE2, BNP and ANP during heart failure predisposes to SARS-CoV-2 infection. ACE2, BNP and ANP therefore could be a novel therapeutic target to prevent the SARS-CoV-2 infection.

Materials and Methods

Study Participants

Patients admitted to Ezhou Central Hospital, Ezhou, China with laboratory-confirmed COVID-19 were included in this retrospective cohort study, which was conducted from January 25, 2020, to March 15, 2020. The patients with COVID-19 enrolled in this study were diagnosed according to World Health Organization interim guidance [15]. The cases without a BNP measurement were excluded. This study was approved by the National Health Commission of China and Shanghai Tenth People's Hospital, Tongji University School of Medicine (Shanghai, China). Written informed consent was waived by the ethics committee of the designated hospital for patients with emerging infectious diseases.

Data Collection

The demographic characteristics, clinical data (comorbidities, laboratory findings, and outcomes), laboratory findings for participants during hospitalization were collected from electronic medical records. Cardiac biomarkers measured on admission were collected, including TNI, CK-MB, and BNP. All data were independently reviewed and entered the computer database by three analysts. Patients were categorized according to the BNP. Acute heart failure (HF) was defined as blood levels of BNP above 100 pg/ml, regardless of cardiovascular disease history and new abnormalities in electrocardiography and echocardiography. The clinical outcomes (i.e., discharges and mortality) were monitored up to March 15, 2020.

PCR-Fluorescence probing based kit (Novel Coronavirus(2019-nCoV) Nucleic Acid Diagnostic Kit, Sansure Biotech, China) was used to extract nucleic acids from clinical sample

and detect the ORF1ab gene (nCovORF1ab) and the N gene (nCoV-NP) according to the manufacturer's instructions. An infection was considered laboratory-confirmed if the nCovORF1ab and nCoV-NP tests both showed positive results.

Statistical Analysis

Descriptive statistics were obtained for all study variables. Continuous data were expressed as mean (SD) or median (interquartile range [IQR]) values. Categorical data were expressed as proportions. All continuous variables were compared using the t-test or the Mann-Whitney U-test if appropriate. In contrast, categorical variables were analyzed for the study outcome by Fisher exact test or $\chi 2$ test. The Pearson correlation coefficient and Spearman rank correlation coefficient were used for liner correlation analysis. Survival analysis between patients with BNP<100 pg/mL and ≥100 pg/mL was conducted by the Kaplan-Meier estimate with p-value generated by the log-rank test. Data were analyzed using SPSS version 25.0 (IBM Corp) or Graphpad Prism 8.0.1 (GraphPad Software, San Diego, CA). For all the statistical analyses, 2-sided $p<0.05$ was considered significant.

scRNA-seq analysis

Data Sources

Adult human heart scRNA-seq datasets were obtained from Gene Expression Omnibus (GEO) under accession codes GSE109816 and GSE121893. Shortly, samples from fourteen healthy donors, six HF patients who were undergoing heart transplantation and two patients with heart failure before and after LV assist device (LVAD) treatment were obtained. The range of donor ages was 21-52 year, with a median age of 45.5 year.

Sequencing data processing

The processed read count matrix was retrieved from existing sources based on previously published data as specified explicitly in the reference. Briefly, Raw reads were processed using the Perl pipeline script supplied by Takara.

Single-cell clustering and identify cell types

The processed read count matrix was imported into R (Version 3.6.2) and converted to a Seurat object using the Seurat R package (Version 3.1.2). Cells that had over 75% UMIs is derived from the mitochondrial genome were discarded. For the remaining cells, gene expression matrices were normalized to total cellular read count using negative binomial regression method implemented in Seurat *SCTransform* function. Cell-cycle scores were calculated using Seurat *CellCycleScoring* function. The Seurat *RunPCA* functions were performed to calculate principal components (PCs). We further corrected the batch effect using Harmony because batch effects among the human heart samples were observed. The *RunUMAP* function with default setting was applied to visualize the first 35 Harmony aligned coordinates. The *FindClusters* function with resolution=0.2 parameter was carried out to cluster cells into different groups. Canonical marker genes were applied to annotate cell clusters into known biological cell types. Monocle 3[16] as used to perform trajectory and pseudotime analysis.

Identification of differential expression genes (DEG)

To identify DEG between two groups, we applied the Seurat *FindMarkers* function with the default parameter of method “MAST” and cells ID from each defined group (e.g. ACE2+ cells vs ACE2- cells in CM1) as input.

Gene function analysis

GSEA (Version 4.03) was used to perform gene ontology (GO) term and pathway enrichment analysis with the Molecular Signatures Database (MSigDB, C2 and C5, Version 7.01).

Results

Clinical Characteristics

The median age of these 91 SARS-CoV-2-infected patients was 66 years (range, 27-89 years), and 54 (59.3%) were male. 46 patients (50.5%) were divided into elevated BNP group (≥100 pg/mL) with median (IQR) level of 299.5 [180.0, 548.0] pg/mL. HF patients have increased ANP and BNP plasma concentrations, which correlates with cardiovascular disease severity. BNP is widely recognized as a diagnostic marker and therapeutic hormone in clinical practice[17]. Patients with higher BNP were older (median age, 79 [44-89] years vs. 62 [27-79] years; p<0.0001). In the higher BNP group, levels of white blood cell (13.05 [6.76, 18.13] 10^9/L) and neutrophil (11.88 [4.83, 16.93] 10^9/L) were significantly higher, while the level of lymphocyte (0.50 [0.27, 0.78] 10^9/L) was significantly lower. Generally, organ impairment was significantly more severe in higher BNP group, including worse liver function indicated by aspartate transaminase (AST, 41.5 [29.0, 64.0], U/L), direct bilirubin (6.6 [4.0, 13.2], μmol/L), and lactate dehydrogenase (LDH, 407.0 [288.0, 599.0], U/L) and worse renal function indicated by eGFR (86.5±44.5, mL/(min*1.73m2) and blood urea nitrogen (BUN, 9.0 [5.2, 15.9], mmol/L). Cardiac injury indicated by troponin I (0.05 [0.03, 0.25], ng/mL) was significant in higher BNP group. Electrolytes disturbance with elevated potassium (4.19 [3.64, 4.70], mmol/L) and decreased calcium (1.97±0.18, mmol/L) level were observed in higher BNP group. Among the coagulation profiles, prothrombin time (PT, 13.9 [12.8, 16.7], s) was

prolonged and D-dimer (6.96 [3.25, 24.2], μg/mL) level was significantly raised. Inflammatory biomarkers, as procalcitonin (1.01 [0.39, 3.51], ng/mL) and hsCRP (18.00 [13.45, 21.50], mg/L), showed a more intense infection in higher BNP group. Blood gas analysis was comparable between groups. Noteworthy, mortality (58.70%) was significantly higher in patients with higher BNP. (Shown in Table 1)

Relationships between BNP level and clinical assessments

Although blood gas analysis was comparable between groups, patients with higher BNP level had a higher incidence of respiratory failure (RF, 31.43%, p=0.0064) (Fig. 1A). BNP level was positively correlated with procalcitonin (r=0.6365, p<0.0001, R2=0.38), neutrophil (r=0.5263, p<0.0001, R2=0.25), and D-dimer (r=0.5824, p<0.0001, R2=0.33), but negatively correlated with lymphocyte (r=-0.5585, p<0.0001, R2=0.29). (Fig. 1B-E). Of note, mortality was significantly increased through a 30-day follow-up in the higher BNP group. (Log-rank p<0.0001) (Fig. 1F).

Integrated analysis of normal and HF conditions at single-cell resolution

To detect the discrepancy between normal and heart failure patients, the schematic of the study was performed according to the description of Wang *et al*[18] . Shortly, the samples of fourteen healthy donors (hereinafter called normal) were obtained. Six HF patients were undergoing heart transplantation and two patients with HF before and after left ventricle assist device (LVAD) treatment (hereinafter called patient). 9767 out of 9994 cells from normal and 4931 out of 4933 cells from patient passed standard quality control and retained

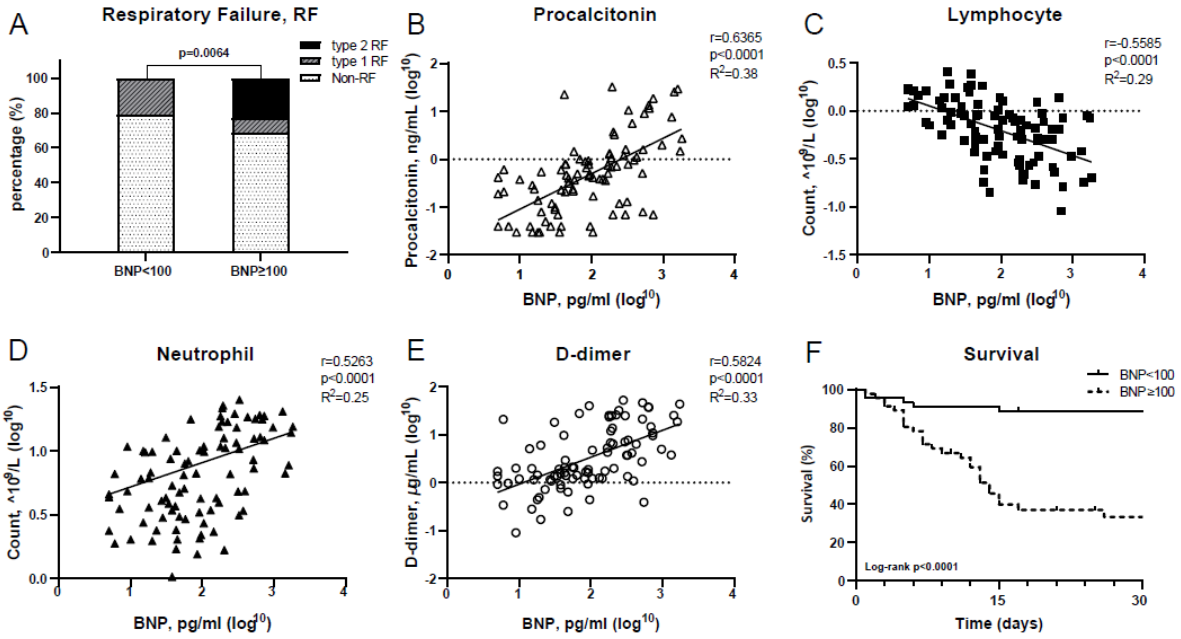

Figure 1. Relationships between BNP level and clinical assessments.

A, the bars were constituted by percentages of non-respiratory failure (RF), type 1 RF, and type 2 RF patients. There were 79.17% patients with non-RF, 20.83% RF1, and no RF2 in BNP<100 pg/mL group, while 68.57% non-RF, 8.57% RF1, and 22.86% RF2 in BNP≥100 pg/mL group. The proportion of groups was significantly different (p=0.0064). **B, C, D and E,** the procalcitonin, neutrophil, and D-dimer level presented a significantly positive correlation with BNP level after log transformation, and lymphocyte presented a negative correlation. **F,** K-M estimate showed the mortality in BNP≥100 pg/mL (dash line) group (58.7%) was significantly higher compared with BNP<100 pg/mL (solid line) group (11.11%) after a 30-day follow-up.

for subsequent analyses. On average, we detected 1649 and 1904 genes in individual cell from normal and patient, respectively. Then, we performed uniform manifold approximation and projection (UMAP) and clustering analysis and grouped the entire population into nine clusters

(Fig. 2A). Dot plot showed the gene expression of known markers for nine clusters, which include: 1) endothelial cells (Cluster 1, PECAM1 and VWF); 2) fibroblasts (Cluster 5, LUM and DCN); 3) smooth muscle cells (Cluster 3, MYH11); 4) NK-T/ monocytes (Cluster 6, CD3G and CD163); 5) granulocytes (Cluster 9, HP, ITLN1); 6) CM2 and 3 subsets (Clusters 2/4/8, MYH6 and NPPA); 7) CM1 and 4 subsets (Clusters 0 and 7, MYH7 and MYL2) (Fig. 2B). Then, UMAP for an individual sample was separately plotted side by side and exhibited the differential distribution of subsets between normal and HF patients. As shown in Fig. 2C, all nine subsets were detected in both normal and patient group. However, different cell type displayed various cell number percentage change between normal and patients. CM1 percentage dramatically decreased from 39.65% to 7.12% ($p<0.0001$), while the percentage of CM4 significantly increased from 0.03% to 7.81% ($p<0.0001$). CM2 and CM3 also increased from 17.70% to 20.08%($p<0.0001$) and 8.27% to 11.56%（$p=0.0005$）respectively.

Cell numbers of endothelial and fibroblasts were also increased from 16.79% to 24.07%($p<0.0001$) and 4.53% to 10.97% ($p=0.0018$) after HF, respectively (Fig. 2D). Their cell percentage changes during HF suggest different cell type has a specific response, especially in cardiomyocytes, endothelial cells and fibroblasts. For each cluster, we calculated the cluster-specific expression genes (marker genes). Left ventricle (LV) marker genes MYL2 and MYL3 were highly expressed in CM1 and 4; so, we termed the subsets CM1 and 4 as LV cardiomyocytes. Left atrium (LA) marker genes MYH6 and MYH7 are highly expressed in CM2 and 3, they were termed as LA cardiomyocytes[19].

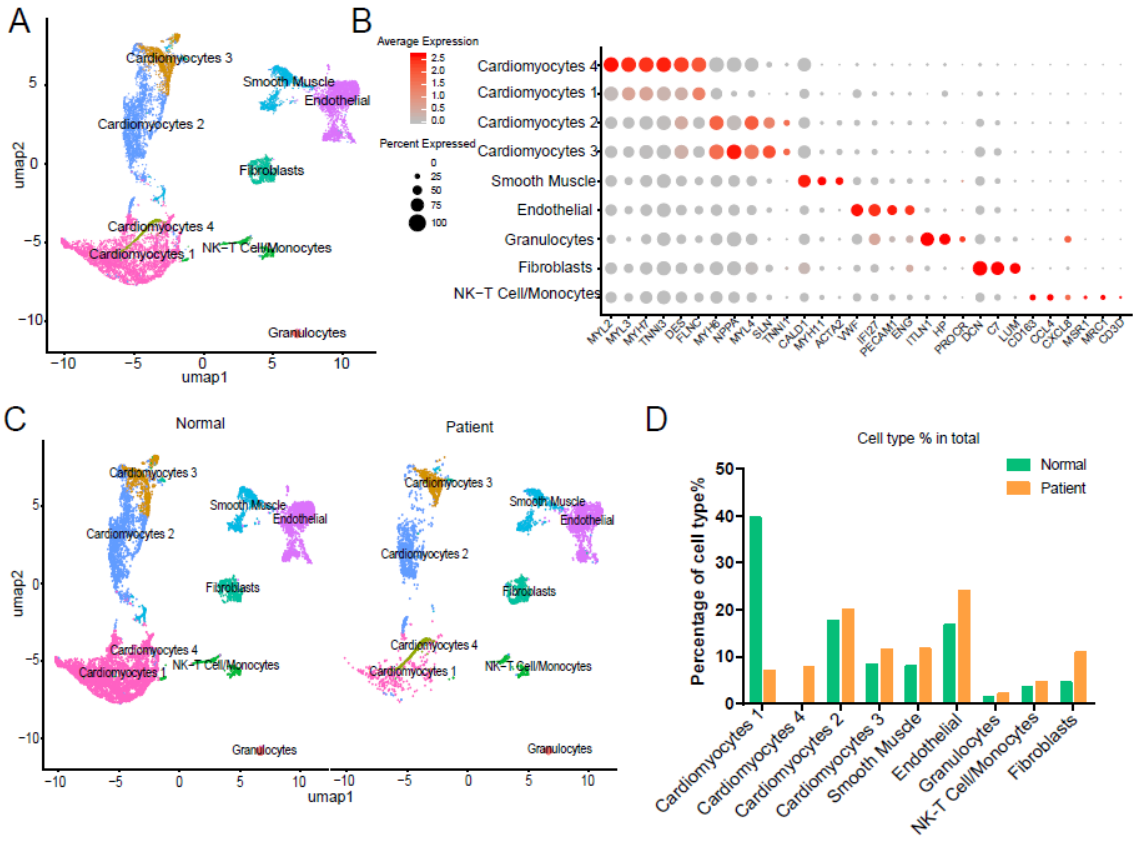

Figure 2. Integrated analysis of normal and HF conditions at single-cell resolution

A, UMAP clustering of 14698 cells isolated from normal and heart failure patients. Each dot represents a single cell. Cell type was annotated by the expression of known marker genes. B, Dot plotting showing gene signature among different clusters, the shadings denotes average expression levels and the sizes of dots denote fractional expression. C, Split views show the 9 subsets in normal and patient group. D, The percentage of cell number for different cell types in normal and patient group.

CMS and Non-CMs (NCMs) shows different characteristics between normal and HF

We compared genes expression of atrial monocytes (CM2&3) and NCMs between normal and patients. We observed that GO term viral genes expression was up-regulated at all atrial

monocytes and NCMs in HF (Supplementary Fig. S1A-F). We previously reported that all atrial monocytes and NCMs have high percentage of ACE2+ cells. These results suggested that all kind of cell type in heart are liable to SARS-CoV-2. In addition, for atrial monocytes of failing heart, GO results showed us that genes related to mitochondrial protein complex and other related to ATP synthesis are up-regulated while genes related to inflammatory response, leukocyte migration, response to interferon-gamma and others related to defend against pathogens are downregulated, indicating failing atrial monocytes is characterized with lower resistance to virus (Supplementary Fig. S1A). From these results, CMs show different characteristics from normal and failing heart, indicating different role in virus infection.

To further determine the relationship between CM1 and CM4, we performed trajectories analysis of the integrated clusters to show the pseudotime of CMs and NCMs. Trajectory and pseudotime results indicated CM4 originated from CM1 (Fig. 3A), which is consistent with our speculation that CM4 is a type of abnormal CM after HF. Then we conducted GSEA analysis (GO and Pathway) on DEG between CM4 and CM1. GO term viral gene expression and pathway influenza infection, infectious diseases and HIV infection were upregulated in CM4 (Fig. 3B and C); but GO term response to virus, defense response to virus, response to interferon gamma and innate immune response, and pathway the adaptive immune response, interferon signaling and interferon-alpha-beta-gamma signaling was down-regulated significantly in CM4 (Fig. 3D and 3E). In summary, these results indicate CM4 is more vulnerable to virus than CM1.

CMs and NCMs have different ACE2 expression pattern

We further investigated ACE2+ cells frequency change of CMs and NCMs in the failing heart by comparing them with normal hearts. Fig. 4A showed that the distribution of ACE2+ cells during HF shifted. Additionally, we calculated the ACE2+ cells frequency across distinct cell subsets of CMs and NCMs. The frequency of ACE2+ cells increased significantly in three of four CMs in HF patients, especially in CM1 and CM4. The proportions rose from 5.55% to 31.05% ($p<0.0001$) and from 0% to 7.01% ($p<0.0001$) respectively. The frequency of ACE2+ cells in CM3 significantly increased from 6.19% to 13.16% ($p<0.0001$), but CM2 didn't change (from 5.55% to 5.66%, $p>0.05$) (Fig. 4B).

In summary, our scRNA-seq results demonstrated that ACE2+ CMs dramatically increased during HF, which suggests that HF patients are more susceptible to SARS-CoV-2 than regular patients. Also, ventricular myocytes had higher percentage of ACE2+ cells than that at atrial myocytes, which indicate that they have different response to SARS-CoV-2. ACE2+ cells percentage in NCMs showed a various pattern, for example, the percentage of ACE2+ cells in fibroblasts ($p<0.0001$) and smooth muscle cells ($p=0.0104$) were decreased. The frequency of ACE2+ cells in immune subsets NK-T Cell/Monocytes and granulocytes increased from 3.77% to 4.85% ($p>0.05$), 2.04% to 5.83% ($p> 0.05$), respectively.

Virus infection-related genes are upregulated in HF patients compared with normal

First, we focused on gene expression dynamics of SARS-CoV-2 entry receptor, ACE2. To further examine the potential role of ACE2+ cells in myocardium infected by SARS-CoV-2, we separated each cell types into two sub-groups (ACE2 positive and ACE2 negative) and called DEGs between these two groups. In ventricular myocytes, *NPPB*, the gene coding

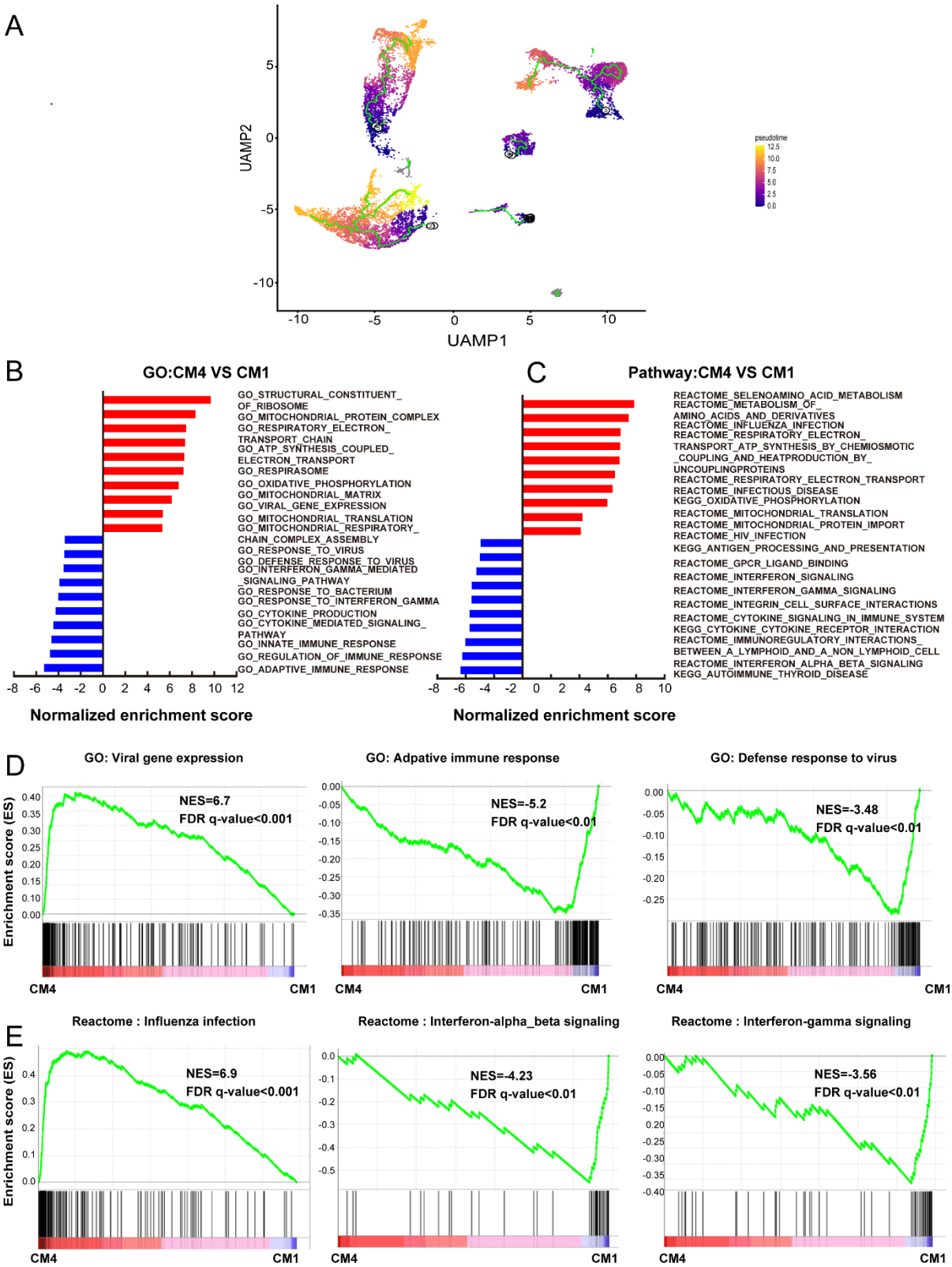

Figure 3. CM4 shows different characteristics with CM1

A, Pseudotime analysis of the nine clusters, the color from purple to yellow denote the different developing stage, and the simultaneous principal curve indicates the pseudo-time stage. **B, C**, GSEA analysis revealed that significant enrichment of GO and pathways for DEGs of CM4 and CM1. **D**, GO enrichment showing GO terms of increased viral gene expression, decreased adaptive immune response and defense response to virus. **E**, Influenza infection signaling pathway is up-regulated, both interferon-alpha-beta signaling and interferon-gamma signaling are down-regulated

BNP and *NPPA* (the gene coding ANP) is the top two upregulated genes with fold change >1.8 in ACE2+ cells. Previous studies reported that ACE2, ANP, BNP, TnT and TnI could make a feedback loop to reserve ejection fraction in HF[20-23] patients . We further studied these ejection fraction preservation genes. Interestingly, we found out that most of them not only are significantly upregulated during HF, but also upregulated in ACE2+ CMs cells (Fig. 4C). To denote their relationship, we built gene regulatory network (GRN) using string (string-db.org). GRN showed that *ACE2*, *NPPA*, *NPPB*, *TNNT1*, *TNNT 2* and *TNNT3* were well connected (Fig. 4D). Based on these co-incidence results, we speculate that these ejection fraction preservation genes may affect virus infection.

Next, we studied the gene expression dynamics of ACE2, *NPPA* and *NPPB* in CMs and NCMs during HF. Both *NPPB* and *NPPA* were co-expressed with ACE2 and significantly up-regulated in CMs during HF (Fig. 5A, 5B). *NPPB* and *NPPA* have different expression pattern. *NPPA* has high expression at atrial myocytes (CM2, 3) and NCMs in normal heart and was significantly upregulated at all CMs (Fig. 5B). *NPPB* has relatively low, but specific expression at atrial myocytes (CM2, 3) in normal heart and significantly upregulated

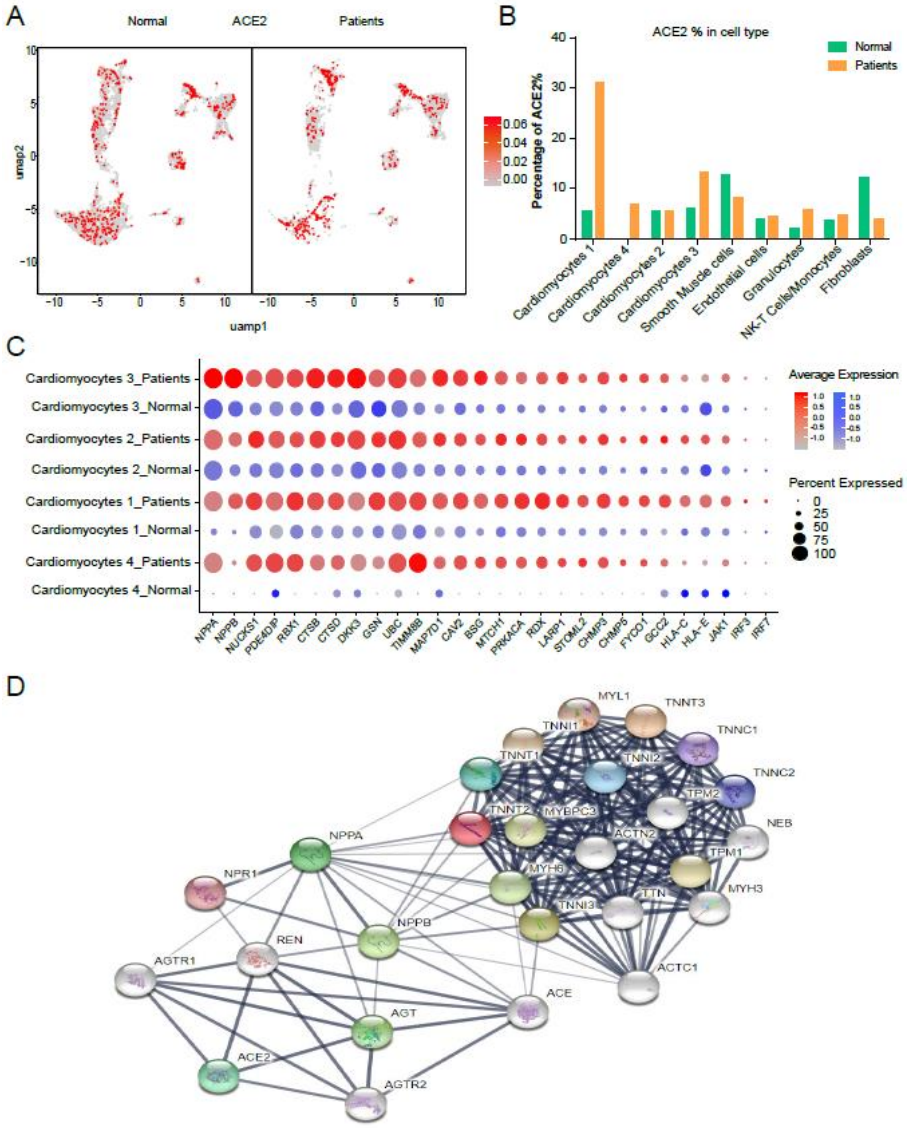

Figure 4. CMs and NCMs have different ACE2 expression pattern

A, UMAP of the CMs and NCMs subsets in normal and HF patients. **B,** Frequency of ACE2+ cells in different cell types. **C,** Gene expression pattern of virus infection-related genes in different subsets of CMs during HF. **D**, Gene regulatory network of ACE2, NPPA, NPPB and TNNT1,2,3.

at all CMs except CM4(Fig. 5A). To our surprise, *NPPB* is barely expressed at CM4. Then, we extended our research to other virus infection-related genes, which involved in virus entry

(BSG, CAV2, CHMP3, CHMP5, STOML2), cysteine proteases cathepsins (CSTB, CSTD, CSTL), virus replication (AKAP9, RDX, MTCH1) and suppression of IFN-γ signaling (LARP1, RBX1 and TIMM8B) (Fig. 5C-F). Genes contributed to virus entry (Fig. 5C,5D, Supplementary Fig. S2A, S2B), virus replication (Fig. 5F) and suppression of IFN-γ signaling (Fig. 5E) were up-regulated at CMs during HF. SARS-CoV-2 entry host CMs requires ACE2 spike protein and protease. It was reported that SARS-CoV-2 can use ACE2 and cellular protease TMPRSS2 for entry into host cells[24].

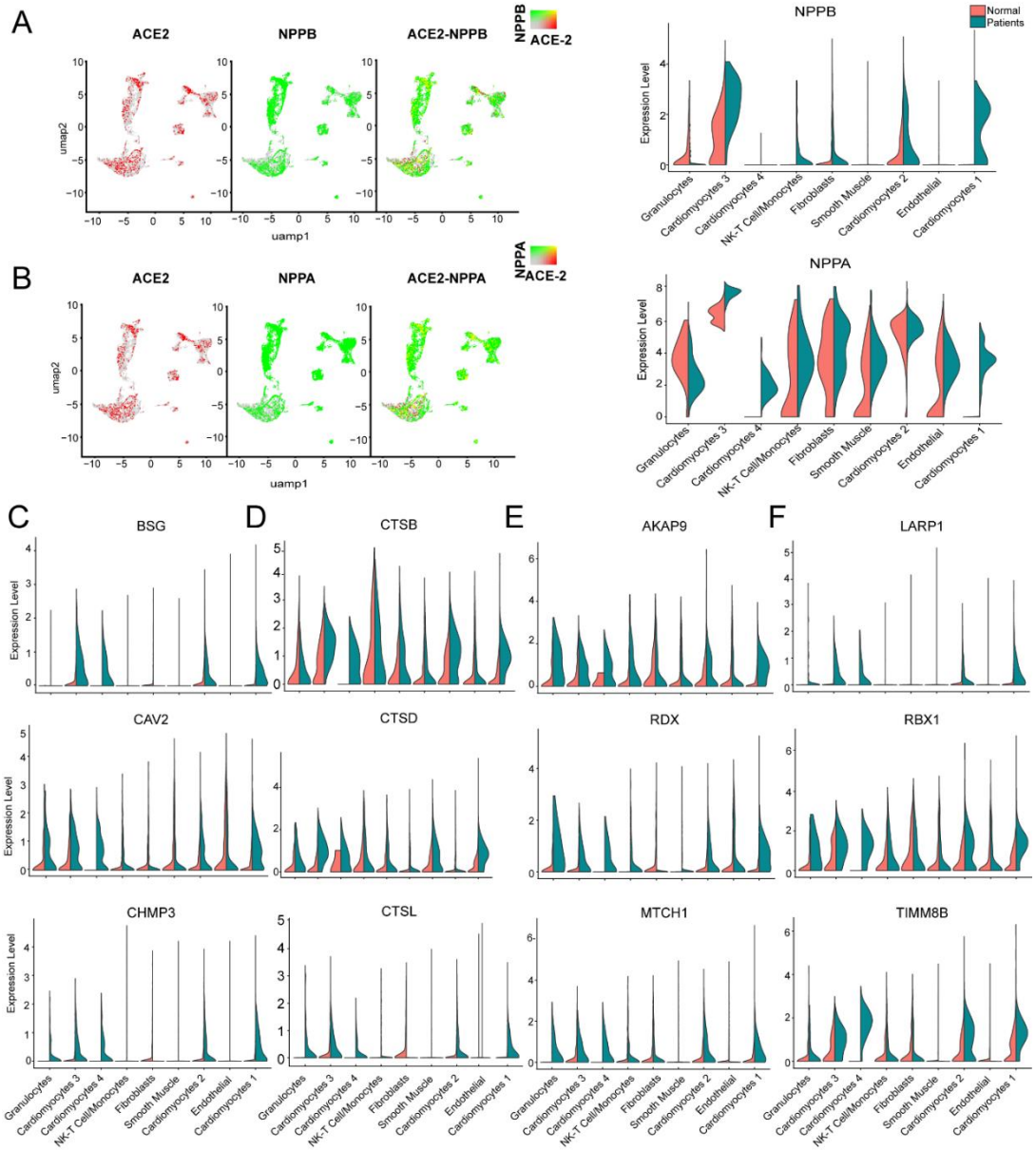

Figure 5. Virus related genes are upregulated in HF patients compared with normal

A, Expression level of ACE2 (red dots), NPPB (green dots) in different clusters, overlapping is shown in the right panel, and the co-expression is shown in yellow dots. Violin plots of the distribution of NPPB between normal and HF patients in different subsets. **B**, Expression level of ACE2 (red dot), NPPA (green dot) in different subsets, overlapping is shown in the right panel, and the co-expression is shown in yellow dots. Violin plots of the distribution of NPPA between normal and HF patients in different subsets. **C**, Violin plots of the distribution of genes (from top to bottom BSG, CAV2, CHMP3) related to viral infection. **D**, Violin plots of the gene expression pattern of CST B/L. **E**, Violin plots of the distribution of genes (from top to bottom AKAP9, RDX, MTCH1) related to IFN-γ signaling pathway. **F**, Violin plots of the distribution of genes (from top to bottom LARP1, RBX1, TIMM8B) on viral replication.

Surprisingly, we barely detected expression of TMPRSS2 in both normal and HF samples (Supplementary Fig. S2C). It was reported that inhibiting both proteases plays an indispensable role in blockade of SARS-CoV viral entry[25] and SARS-CoV-2 can use them to prime in cell lines[24]. So, we investigated gene expression dynamics of the endosomal cysteine proteases cathepsins and found out that CTSB, CTSD and CTSL were up-regulated significantly in CMs during HF (Fig. 5D). We speculate that virus mainly uses ACE2-CTSB/L axis entry into host cells. The above results imply that Heart dysfunction or HF patients are more vulnerable to SARS-CoV-2.

Thrombosis is the main cause accentuate illness in severe patients[26]. Tissue factor

(TF/CD142) activation cause thrombus formation on atherosclerotic plaques coded by F3[27]. We investigated the expression dynamics of genes related to signal blood clotting. F3 was co-expressed with ACE2 and significantly up-regulated in CM3 and CM1 during HF (Supplementary Fig. S2D) which indicated that HF patient may possess increased risk of blood clot.

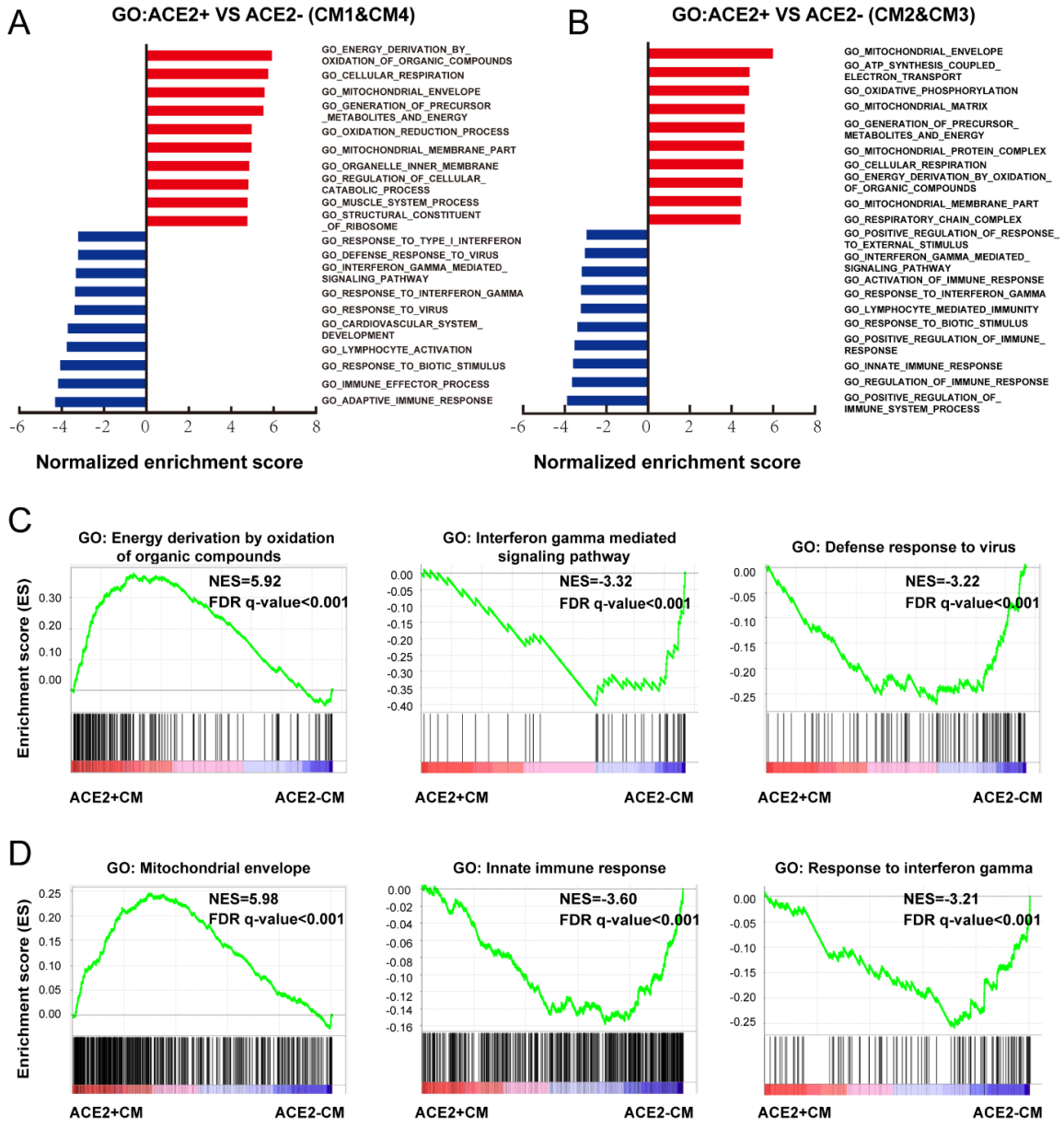

Figure 6. Characteristics of ACE2-positive ventricular and atrial myocytes.

346 **A,** GO analysis revealed that significant enrichment of biological pathways from comparison
347 of ACE2+ ventricular myocytes and ACE2- ventricular myocytes. **B,** GO analysis revealed that
348 significant enrichment of biological pathways from comparison of ACE2+ atrial myocytes and
349 ACE2- atrial myocytes. **C,** GO plots showing GO terms of increased energy derivation by
350 oxidation of organic compounds (left), decreased interferon gamma mediated signaling
351 pathway (median) and down-regulated defense response to virus (right). **D,** GO enrichment
352 plots showing GO terms of increased mitochondrial envelope (left), decreased innate immune
353 response (median) and down-regulated innate immune response (right). The NES and false
354 discovery rate (FDR) were showed in panel.

355 **Characteristics of ACE2 positive ventricular and atrial myocytes**

356 We conducted GSEA analysis on DEGs of cells between ACE2+ and ACE2- in ventricular
357 myocytes (CM1 and CM4) (Fig.6A, Supplementary Fig. S3A). GO term associated with energy
358 consumption (Fig. 6A), energy derivation by oxidation (Fig. 6C), and pathway influenza
359 infection (Supplementary Fig. S3C) and infectious disease (Fig. S3A) were positively enriched
360 in ACE2+ cells. In contrast, GO terms interferon gamma mediated signaling pathway, defense
361 response to virus and pathway interferon-alpha_beta signaling and interferon signaling were
362 negatively enriched in ACE2+ cells (Fig. 6C, Supplementary Fig. S3C).

363 Furthermore, we performed GSEA analysis on DEGs of cells between ACE2+ and ACE2-
364 in atrial myocytes (CM2 and CM3) (Fig. 6B, Supplementary Fig. S3B). GO terms associated
365 with energy consumption, mitochondrial envelope, ATP synthesis coupled electron transport,
366 oxidative phosphorylation and pathway cardiac muscle contraction, respiratory electron
367 transport were positively enriched (Fig. 6B, 6C, Supplementary Fig. S3B, S3C). On contrary,

GO terms and pathways associated with innate immune response, response to interferon gamma, interferon gamma signaling and interferon-alpha_beta signaling were negatively enriched which shared the same trend as ventricular myocytes (Fig. 6D, Supplementary Fig. S3D). ACE2+ CMs are characterized with capacity of reduced immuno-regulatory effect and have more energy consumption compared with ACE2- CMs. Moreover, we also identified DEGs between ACE2+ NCMs and ACE2- NCMs and GSEA analysis (Supplementary Fig. S4). Interestingly, pathways associated with infectious disease was positively enriched in NCMs, except for NK-T Cells/Monocytes. GO terms associated with mitochondrial matrix and ATP synthesis were positively enriched in smooth muscle cells, NK-T Cells/Monocytes and fibroblasts, which is consistent with observation at CMs. GO term associated with muscle structure and function (Supplementary Fig. S4A, S4E) and leukocyte mediated immunity were negatively enriched in ACE2+ cells of smooth muscle

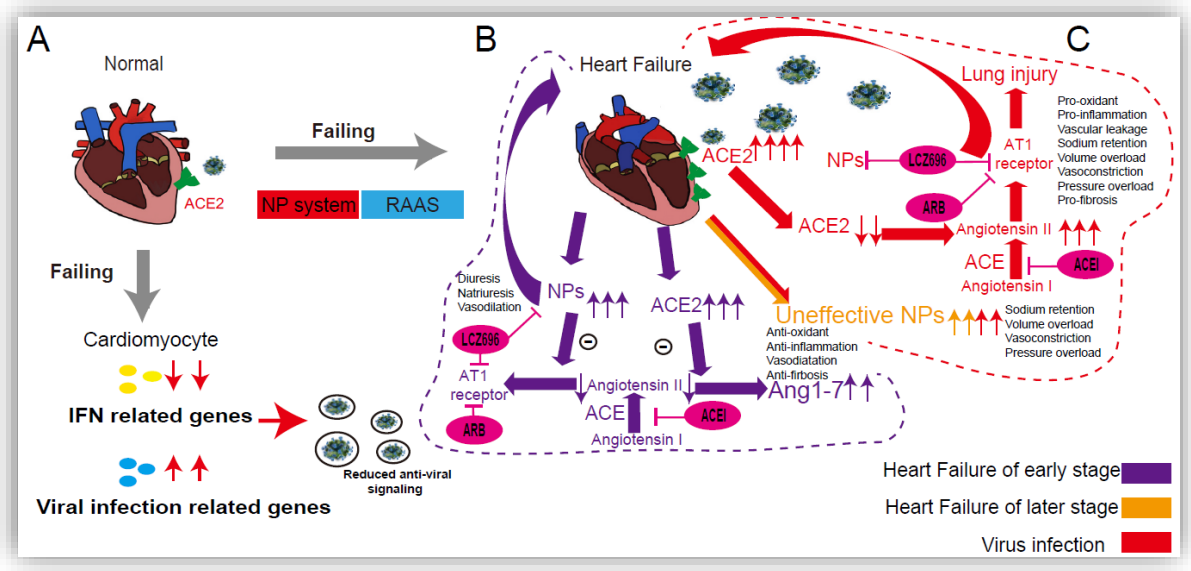

Figure 7. Conceptual Schematic diagram highlighting the central role of SARS-CoV-2 and the natriuretic peptide, Renin-Angiotensin-Aldosterone system in the potentially

deleterious (red) and protective (purple) effects.

A, scRNA-seq analysis detected the down-regulated IFN related genes and up-regulated viral infection related genes during HF, which imply reduced anti-viral signaling. **B,** Schematic diagram showed the process during heart failure in the early stage and later stage noted in purple and orange, respectively. **C,** The process under virus infection was noted in red to speculate the underlying relationship for the higher susceptibility and worse prognosis in HF. Oval circles and bars indicated the potential drug and targets.

cells, fibroblasts, and endothelial cells (Supplementary Fig. S4B). GO term associated with viral expression is positively enriched in ACE2+ granulocytes, while GO term associated with immunocyte mediated immunity is negatively enriched in ACE2+ granulocytes and ACE2+ NK-T Cells/Monocytes which indicates their dysfunctions to fight against pantheons (Supplementary Fig. S4C, S4D).

Discussion

Our clinical data indicates that patients with high BNP (≥100 pg/mL) were more likely to have complications such as liver and kidney injury resulting in a poor prognosis. This is the first study, at single-cell level, to systematically investigate ACE2 and other virus entry related genes expression dynamics of CMs and NCMs in both normal heart and HF patients. In normal heart, most of cell types of CMs and NCMs were detected high percentage of ACE2+ cells comparing with it in the lung, which indicates heart may be infected if exposed to SARS-CoV-2. Chen *et.al.* reported that the pericytes (with marker genes ABCC9 and KCNJ8), but not the cardiomyocyte were ACE2+ cells in normal hearts[28]. According to our scRNA-seq analysis,

most cell types in the normal human heart, including CMs, smooth muscle cells, endothelial, fibroblasts and immune cells have relatively high levels of ACE2 expression. They applied single nucleus RNA-seq to their normal heart samples, which capture much fewer transcripts than the SMART-seq using whole-cell as input. Considering the limitation of their technology, our scRNA-Seq data is more comprehensive and recapitulates the real state of cells.

In the presence of cardiac dysfunction, not only the proportion of ACE2+ cardiomyocytes, especially ventricular myocytes, was dramatically increased in HF patients, but also the expression level of ACE2+ cells are significantly enhanced in cardiomyocytes, especially the ventricular myocytes as well (Fig. 4B). In our study, we have done two kinds of comparison for each type of CMs: 1) DEGs between failing CMs and normal cells, 2) DEG between ACE2+ CMs with ACE- CMs. Interestingly, following GSEA analysis (GO and pathway) of DEGs for these two kinds of comparisons achieved consistent results, in which GO term/Pathway associated with virus infection and virus genes expression were positively enriched, but defense to virus, secretion of IFN and activation of immune system were negatively enriched in CMs (Fig. 3B,3C, 6A, 6B). Our results suggest that patients with heart dysfunction or HF may have a higher susceptibility to SARS-CoV-2 infection (Fig. 7A).

The natriuretic peptide system (NPS), including ANP and BNP play an important role in chronic heart failure by synergizing with the renin-angiotensin-aldosterone system (RAAS) and sympathetic nervous system (SNS)[29]. In the early stage of heart failure, NPs are released to promote diuresis, natriuresis and vasodilation, which is critical for the maintenance of intravascular volume homeostasis (Fig, 7B) [21]. Meanwhile, ACE2 opposes the molecular and cellular effects of Ang II by converting Ang II into Ang 1-7 which acts as a vasodilator and

exerts protective effects in the cardiovascular system as well (Fig, 7B) [20]. However, along with heart failure progresses, the release of functional and effective NPs is blocked, exhibited increasing NPs but ineffective levels in plasma, further result in the heart dysfunction[30]. Previous studies have established that failed CMs could secrete poorly active prohormones like pro-ANP and pro-BNP[31]. COVID-19 patients SARS-CoV-2 infection could cause a series of symptoms related to myocardial injury, including cardiac dysfunction. So, we speculate NPs may play an important role in virus infection and following heart injury.

Patients suffered heart dysfunction and secreting ineffective NPs including pro-ANP and pro-BNP may have different scenario. Our scRNA-seq analysis results indicate that patients with heart dysfunction or HF have more ACE2+ CMs and higher expression ACE2 and have a higher susceptibility to SARS-CoV-2 infection. It was reported that SARS-CoV led to down-regulation of ACE2 and then up-regulate its substrates Ang II, which caused more severe lung injury in mice[32, 33.] Similar reaction axis was found in SARS-CoV-2 between ACE2 and Ang II, and the accumulation of Ang II may further lead to vascular effectiveness in other organs such as lung and kidney [34]. Moreover, BNP as an early responsive gene to stress in the myocardium than ANP[35], whose expression level was increased significantly when stimulated by Ang II in human[36, 37]. In our study, DEG between ACE2+ and ACE2- ventricular myocytes showed both BNP and ANP were top two genes up-regulated. We searched ENCODE database for transcription factor (TF) binding sites in promoter of ACE2, ANP and BNP. Among the top five TFs, they share top two TFs (AP1 and c-Jun), which imply that they are probably be co-regulated during HF. For Patients suffered heart dysfunction and secreting ineffective NPs, if their hearts are infected by SARS-CoV-2, they don't have enough effective NPs and Ang1-7

449 to preserve ejection fraction; so more heart cell damage and more ACE2+ cells will be expected,
450 which in versa cause more heart cells being susceptibility to SARS-CoV-2 infection (Fig7C).
451 Finally, ACE2, ineffective NP, virus and Ang II formed a positive feedback loop, which lead
452 to severe outcome. In summary, there have two scenarios for COVID-19 patients with heart
453 dysfunction: 1) For patients have normal level of effective NPs, they may benefit from
454 protective effects of NPs and ACE2 negative feedback loop and have better prognosis (Fig.
455 7B). 2) For patients have deficient level of effective NPs, a positive feedback loop may be
456 formed with ACE2, ineffective NP, virus, which cause worse prognosis (Fig. 7C). Drug ACEI
457 or ARBs can break this positive feedback loop by reducing Ang II. They maybe benefit from
458 these kinds of drugs, including ACEI, ARBs and LCZ696/Entresto. Ratio of effective versus
459 ineffective NPs may be the very important factor to make decision whether patients can take
460 these drugs or not.
461

462 ## Supplementary material

463 Supplementary material is available at European Heart Journal online.

464 ## Acknowledgements

465 We thank Xinli Hu for helpful discussion and review of the manuscript. Also, we also want to
466 thank Yuxi Sun, Teng Ma and Yawei Xu for helpful discussion.

467 ## Funding

468 This study was supported by grants from National Natural Science Foundation of China (No.
469 81770391 to Dachun Xu)

470 **Conflict of interest**: None of the authors have any relevant conflicts of interest to declare.

Reference

1. Huang C, Wang Y, Li X, Ren L, Zhao J, Hu Y, Zhang L, Fan G, Xu J, Gu X, Cheng Z, Yu T, Xia J, Wei Y, Wu W, Xie X, Yin W, Li H, Liu M, Xiao Y, Gao H, Guo L, Xie J, Wang G, Jiang R, Gao Z, Jin Q, Wang J, Cao B. Clinical features of patients infected with 2019 novel coronavirus in Wuhan, China. The Lancet 2020;**395**(10223):497–506.
2. COVID-19 Dashboard by the Center for Systems Science and Engineering(CSSE) at Johns Hopkins.
3. Chen N, Zhou M, Dong X, Qu J, Gong F, Han Y, Qiu Y, Wang J, Liu Y, Wei Y, Xia Ja, Yu T, Zhang X, Zhang L. Epidemiological and clinical characteristics of 99 cases of 2019 novel coronavirus pneumonia in Wuhan, China: a descriptive study. The Lancet 2020;**395**(10223):507–513.
4. Wang D, Hu B, Hu C, Zhu F, Liu X, Zhang J, Wang B, Xiang H, Cheng Z, Xiong Y, Zhao Y, Li Y, Wang X, Peng Z. Clinical Characteristics of 138 Hospitalized Patients With 2019 Novel Coronavirus-Infected Pneumonia in Wuhan, China. JAMA 2020.
5. Shi S, Qin M, Shen B, Cai Y, Liu T, Yang F, Gong W, Liu X, Liang J, Zhao Q, Huang H, Yang B, Huang C. Association of Cardiac Injury With Mortality in Hospitalized Patients With COVID-19 in Wuhan, China. JAMA cardiology 2020.
6. Guo T, Fan Y, Chen M, Wu X, Zhang L, He T, Wang H, Wan J, Wang X, Lu Z. Cardiovascular Implications of Fatal Outcomes of Patients With Coronavirus Disease 2019 (COVID-19). JAMA cardiology 2020.
7. Lu R, Zhao X, Li J, Niu P, Yang B, Wu H, Wang W, Song H, Huang B, Zhu N, Bi Y, Ma X, Zhan F, Wang L, Hu T, Zhou H, Hu Z, Zhou W, Zhao L, Chen J, Meng Y, Wang J, Lin Y, Yuan J, Xie Z, Ma J, Liu WJ, Wang D, Xu W, Holmes EC, Gao GF, Wu G, Chen W, Shi W, Tan W. Genomic characterisation and epidemiology of 2019 novel coronavirus: implications for virus origins and receptor binding. The Lancet 2020;**395**(10224):565–574.
8. Zhou P, Yang X-L, Wang X-G, Hu B, Zhang L, Zhang W, Si H-R, Zhu Y, Li B, Huang C-L, Chen H-D, Chen J, Luo Y, Guo H, Jiang R-D, Liu M-Q, Chen Y, Shen X-R, Wang X, Zheng X-S, Zhao K, Chen Q-J, Deng F, Liu L-L, Yan B, Zhan F-X, Wang Y-Y, Xiao G-F, Shi Z-L. A pneumonia outbreak associated with a new coronavirus of probable bat origin. Nature 2020;**579**(7798):270–273.
9. Zou X, Chen K, Zou J, Han P, Hao J, Han Z. Single-cell RNA-seq data analysis on the receptor ACE2 expression reveals the potential risk of different human organs vulnerable to 2019-nCoV infection. Frontiers of medicine 2020.
10. Qi F, Qian S, Zhang S, Zhang Z. Single cell RNA sequencing of 13 human tissues identify cell types and receptors of human coronaviruses. Biochemical and biophysical research communications 2020.
11. Xu X, Chen P, Wang J, Feng J, Zhou H, Li X, Zhong W, Hao P. Evolution of the novel coronavirus from the ongoing Wuhan outbreak and modeling of its spike protein for risk of human transmission. Science China. Life sciences 2020;**63**(3):457–460.
12. He S, Wang L, Liu Y, Li Y, Chen H, Xu J, Peng W, Lin G, Wei P, Li B, Xia X, Wang D, BEI J-X, He X, Guo Z. *Single-cell transcriptome profiling an adult human cell atlas of 15 major organs*; 2020.
13. Patel VB, Zhong J-C, Grant MB, Oudit GY. Role of the ACE2/Angiotensin 1-7 Axis of the Renin-Angiotensin System in Heart Failure. Circulation research 2016;**118**(8):1313–1326.
14. Zheng Y-Y, Ma Y-T, Zhang J-Y, Xie X. COVID-19 and the cardiovascular system. Nature reviews. Cardiology 2020.
15. World Health Organization interim guidance.
16. Qiu X, Mao Q, Tang Y, Wang L, Chawla R, Pliner HA, Trapnell C. Reversed graph embedding resolves

513 complex single-cell trajectories. Nat Methods 2017;**14**(10):979-982.
514 17. Boerrigter G, Costello-Boerrigter LC, Burnett JC. Natriuretic peptides in the diagnosis and
515 management of chronic heart failure. Heart failure clinics 2009;**5**(4):501-514.
516 18. Wang L, Yu P, Zhou B, Song J, Li Z, Zhang M, Guo G, Wang Y, Chen X, Han L, Hu S. Single-cell
517 reconstruction of the adult human heart during heart failure and recovery reveals the cellular landscape
518 underlying cardiac function. Nature cell biology 2020;**22**(1):108–119.
519 19. Lu ZQ, Sinha A, Sharma P, Kislinger T, Gramolini AO. Proteomic analysis of human fetal atria and
520 ventricle. Journal of proteome research 2014;**13**(12):5869–5878.
521 20. Patel VB, Zhong JC, Grant MB, Oudit GY. Role of the ACE2/Angiotensin 1-7 Axis of the Renin-
522 Angiotensin System in Heart Failure. Circ Res 2016;**118**(8):1313-26.
523 21. Kuhn M. Cardiac actions of atrial natriuretic peptide: new visions of an old friend. Circ Res
524 2015;**116**(8):1278-80.
525 22. Linke WA, Hamdani N. Gigantic business: titin properties and function through thick and thin.
526 Circulation research 2014;**114**(6):1052-1068.
527 23. Takimoto E. Cyclic GMP-dependent signaling in cardiac myocytes. Circulation journal : official journal
528 of the Japanese Circulation Society 2012;**76**(8):1819-1825.
529 24. Hoffmann M, Kleine-Weber H, Schroeder S, Krüger N, Herrler T, Erichsen S, Schiergens TS, Herrler G,
530 Wu N-H, Nitsche A, Müller MA, Drosten C, Pöhlmann S. SARS-CoV-2 Cell Entry Depends on ACE2 and
531 TMPRSS2 and Is Blocked by a Clinically Proven Protease Inhibitor. Cell 2020.
532 25. Kawase M, Shirato K, van der Hoek L, Taguchi F, Matsuyama S. Simultaneous treatment of human
533 bronchial epithelial cells with serine and cysteine protease inhibitors prevents severe acute respiratory
534 syndrome coronavirus entry. Journal of virology 2012;**86**(12):6537-6545.
535 26. Moore BJB, June CH. Cytokine release syndrome in severe COVID-19. Science (New York, N.Y.) 2020.
536 27. Toschi V, Gallo R, Lettino M, Fallon JT, Gertz SD, Fernández-Ortiz A, Chesebro JH, Badimon L,
537 Nemerson Y, Fuster V, Badimon JJ. Tissue factor modulates the thrombogenicity of human atherosclerotic
538 plaques. Circulation 1997;**95**(3):594-599.
539 28. Chen L, Li X, Chen M, Feng Y, Xiong C. The ACE2 expression in human heart indicates new potential
540 mechanism of heart injury among patients infected with SARS-CoV-2. Cardiovascular research 2020.
541 29. Diez J. Chronic heart failure as a state of reduced effectiveness of the natriuretic peptide system:
542 implications for therapy. Eur J Heart Fail 2017;**19**(2):167-176.
543 30. Volpe M, Carnovali M, Mastromarino V. The natriuretic peptides system in the pathophysiology of
544 heart failure: from molecular basis to treatment. Clinical Science 2015;**130**(2):57-77.
545 31. Niederkofler EE, Kiernan UA, O'Rear J, Menon S, Saghir S, Protter AA, Nelson RW, Schellenberger U.
546 Detection of endogenous B-type natriuretic peptide at very low concentrations in patients with heart failure.
547 Circulation. Heart failure 2008;**1**(4):258-264.
548 32. Kuba K, Imai Y, Rao S, Gao H, Guo F, Guan B, Huan Y, Yang P, Zhang Y, Deng W, Bao L, Zhang B, Liu
549 G, Wang Z, Chappell M, Liu Y, Zheng D, Leibbrandt A, Wada T, Slutsky AS, Liu D, Qin C, Jiang C, Penninger
550 JM. A crucial role of angiotensin converting enzyme 2 (ACE2) in SARS coronavirus-induced lung injury. Nat
551 Med 2005;**11**(8):875-9.
552 33. Acanfora D, Ciccone MM, Scicchitano P, Acanfora C, Casucci G. Neprilysin inhibitor-angiotensin II
553 receptor blocker combination (sacubitril/valsartan): rationale for adoption in SARS-CoV-2 patients. Eur
554 Heart J Cardiovasc Pharmacother 2020.
555 34. Muthiah Vaduganathan MD, M.P.H., Orly Vardeny, Pharm.D., Thomas Michel, M.D., Ph.D., , John J.V.
556 McMurray MD, Marc A. Pfeffer, M.D., Ph.D., and Scott D. Solomon, M.D. Renin–Angiotensin–Aldosterone

System Inhibitors in Patients with Covid-19. The NEW ENGLAND JOURNAL of MEDICINE 2020;**382**:1653-1659.

35. Nakagawa O, Ogawa Y, Itoh H, Suga S, Komatsu Y, Kishimoto I, Nishino K, Yoshimasa T, Nakao K. Rapid transcriptional activation and early mRNA turnover of brain natriuretic peptide in cardiocyte hypertrophy. Evidence for brain natriuretic peptide as an "emergency" cardiac hormone against ventricular overload. J Clin Invest 1995;**96**(3):1280-7.

36. de Lemos JA, McGuire DK, Drazner MH. B-type natriuretic peptide in cardiovascular disease. The Lancet 2003;**362**(9380):316-322.

37. Holubarsch CJF. Gene Expression of Brain Natriuretic Peptide in Isolated Atrial and Ventricular Human Myocardium : Influence of Angiotensin II and Diastolic Fiber Length. Circulation 2000;**102**(25):3074-3079.

Table 1. Comparison of COVID-19 patient characteristics between BNP groups.

Parameters	Total (N=91)	BNP<100 (N=45)	BNP≥100 (N=46)	p value
Age, yrs	66 (55.5, 73.0)	62.0 (46.0, 69.0)	79.0 (63.5, 79.0)	**<0.0001***
Male, n (%)	54 (59.3)	23 (51.1)	31 (67.4)	0.11
Complete blood cell count, 10^9/L				
White blood cell	7.99 (4.59, 13.31)	6.28 (4.04, 8.38)	13.05 (6.76, 18.13)	**<0.0001***
Neutrophil	6.6 (3.43, 12.32)	4.29 (2.74, 6.67)	11.88 (4.83, 16.93)	**<0.0001***
Lymphocyte	0.71 (0.38, 1.09)	0.98 (0.62, 1.47)	0.50 (0.27, 0.78)	**<0.0001***
Liver and renal function				
Alanine transaminase, U/L	30.0 (18.5, 52.5)	27.0 (19.0, 49.0)	32.0 (18.0, 64.0)	0.5783
Aspartate transaminase, U/L	37.0 (23.0, 55.0)	30.0 (20.0, 51.0)	41.5 (29.0, 64.0)	**0.0299***
TBIL, μmol/L	14.1 (9.5, 21.7)	11.8 (9.1, 17.8)	15.2 (10.1, 24.4)	0.1216
Direct bilirubin, μmol/L	5.3 (3.4, 9.8)	4.1 (3.0, 6.5)	6.6 (4.0, 13.2)	**0.0047***
Lactate dehydrogenase, U/L	315.0 (179.5, 470.5)	185.0 (154.0, 352.0)	407.0 (288.0, 599.0)	**<0.0001***
eGFR, mL/(min*1.73m^2)	105.6±47.0	121.1±41.6	86.5±44.5	**0.0003***
Blood urea nitrogen, mmol/L	5.7 (3.9, 11.1)	4.5 (3.2, 5.8)	9.0 (5.2, 15.9)	**<0.0001***
Uric acid, μmol/L	234.0 (183.5, 305.5)	235.0 (184.0, 305.0)	230.5 (182.0, 310.0)	0.9494
Cardiac biomarker				
Troponin-I, ng/mL	0.01 (0.01, 0.06)	0.01 (0.01, 0.01)	0.05 (0.03, 0.25)	**<0.0001***
Electrolytes				
Potassium, mmol/L	4.04 (3.64, 4.40)	3.87 (3.56, 4.27)	4.19 (3.64, 4.70)	**0.0354***
Sodium, mmol/L	139.0 (136.0, 142.0)	139.0 (135.0, 141.0)	139.0 (136.0, 145.0)	0.2992
Chloride, mmol/L	102.0 (98.5, 106.0)	103.0 (100.0, 106.0)	101.5 (98.0, 106.0)	0.6473
Calcium, mmol/L	2.03±0.18	2.09±0.16	1.97±0.18	**0.0018***
Coagulation profiles				
Prothrombin time, s	13.4 (12.4, 14.9)	13.0 (12.0, 13.8)	13.9 (12.8, 16.7)	**0.0030***
APTT, s	35.5 (31.8, 39.8)	35.1 (32.4, 38.9)	35.5 (30.7, 42.5)	0.6165
Fibrinogen, g/L	3.39 (2.31, 4.77)	3.39 (2.31, 5.09)	3.40 (2.35, 5.87)	0.8567
D-dimer, μg/mL	2.03 (1.22, 1.00)	1.37 (0.83, 1.99)	6.96 (3.25, 24.20)	**<0.0001***
Inflammatory biomarkers				
Procalcitonin, ng/mL	0.45 (0.12, 1.12)	0.23 (0.04, 0.49)	1.01 (0.39, 3.51)	**<0.0001***

570

571

hsCRP, mg/L	13.80 (5.74, 20.50)	6.09 (1.52, 15.86)	18.00 (13.45, 21.50)	**<0.0001***
Blood gas analysis				
PaO_2, mmHg	71.0 (57.8, 92.0)	78.5 (57.5, 104.5)	68,5 (56.5, 86.0)	0.4867
$PaCO_2$, mmHg	41.0 (34,.0 48.8)	39.5 (33.5, 43.5)	42.5 (34.0, 57.9)	0.1589
Lactic acid, mmol/L	1.95 (1.40, 2.40)	1.80(1.30, 2.15)	2.00 (1.60, 2.75)	0.1634
BNP, pg/mL	92.0 (32.5, 299.5)	34.0 (15.0, 48.0)	299.5 (180.0, 548.0)	**<0.0001***
Death, n (%)	32 (35.16)	5 (11.11)	27 (58.70)	**<0.0001***

Continuous variables are presented as means±SD if conform normal distribution or median with interquartile range if not. Categorical variables are presented as percentage (%).

* Significant p value (<0.05).

TBIL denotes total bilirubin, eGFR estimated glomerular filtration rate (calculated by MDRD formula), APTT activated partial thromboplastin time, hsCRP high-sensitive C-reactive protein, BNP B-type natriuretic peptide.

572

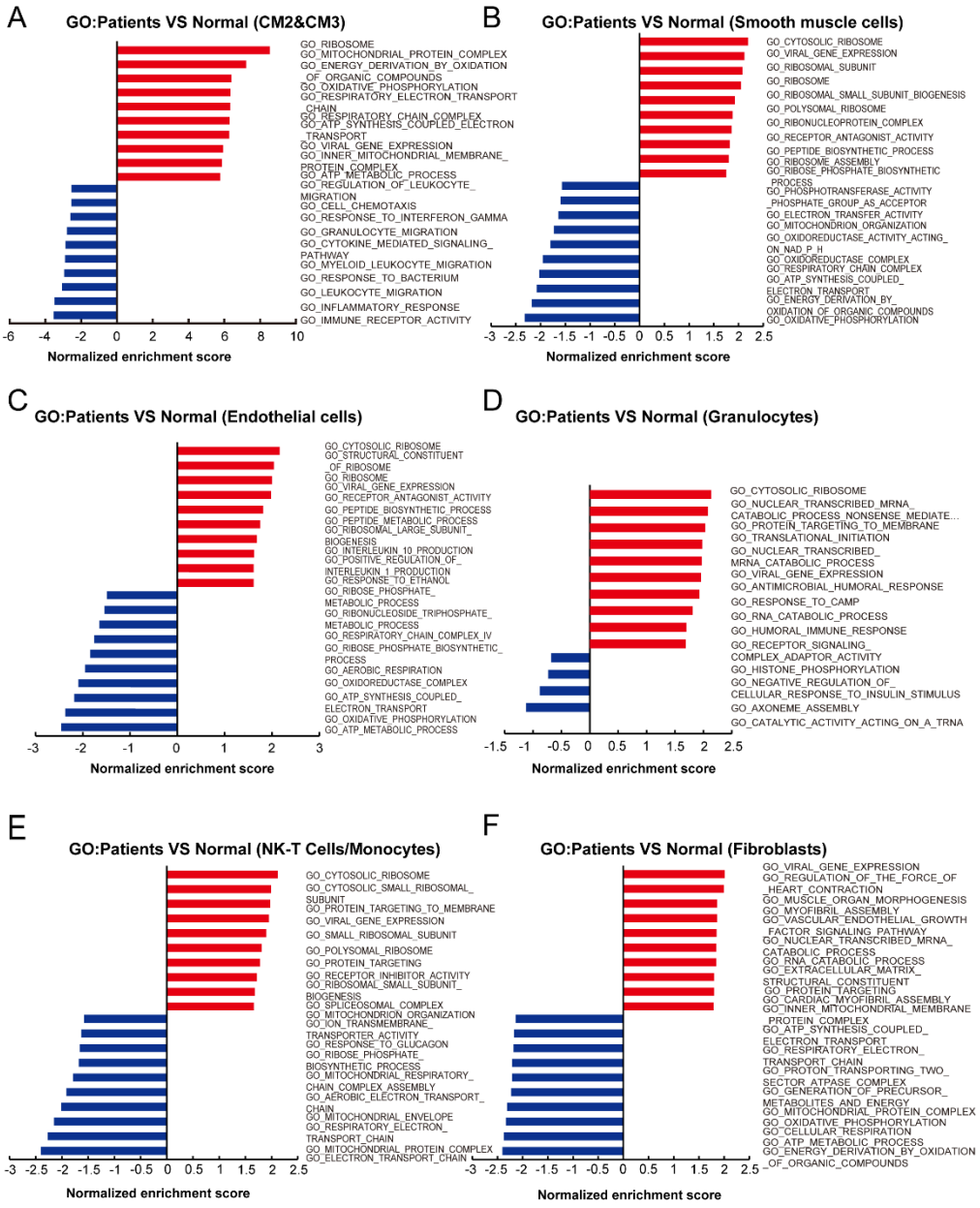

Supplemental Figure. 1. Enrichment of biological pathway in different subsets from comparison of HF patients and normal (related to Fig. 3)

A-F, GO analysis revealed that significant enrichment of biological pathway from comparison of HF patients and normal in different subsets. **A**, CM2 and CM3 subsets. **B**, Smooth muscle cells. **C**, endothelial cells. **D**, Granulocytes. **E**, NK-T cells/Monocytes. **F**, Fibroblasts.

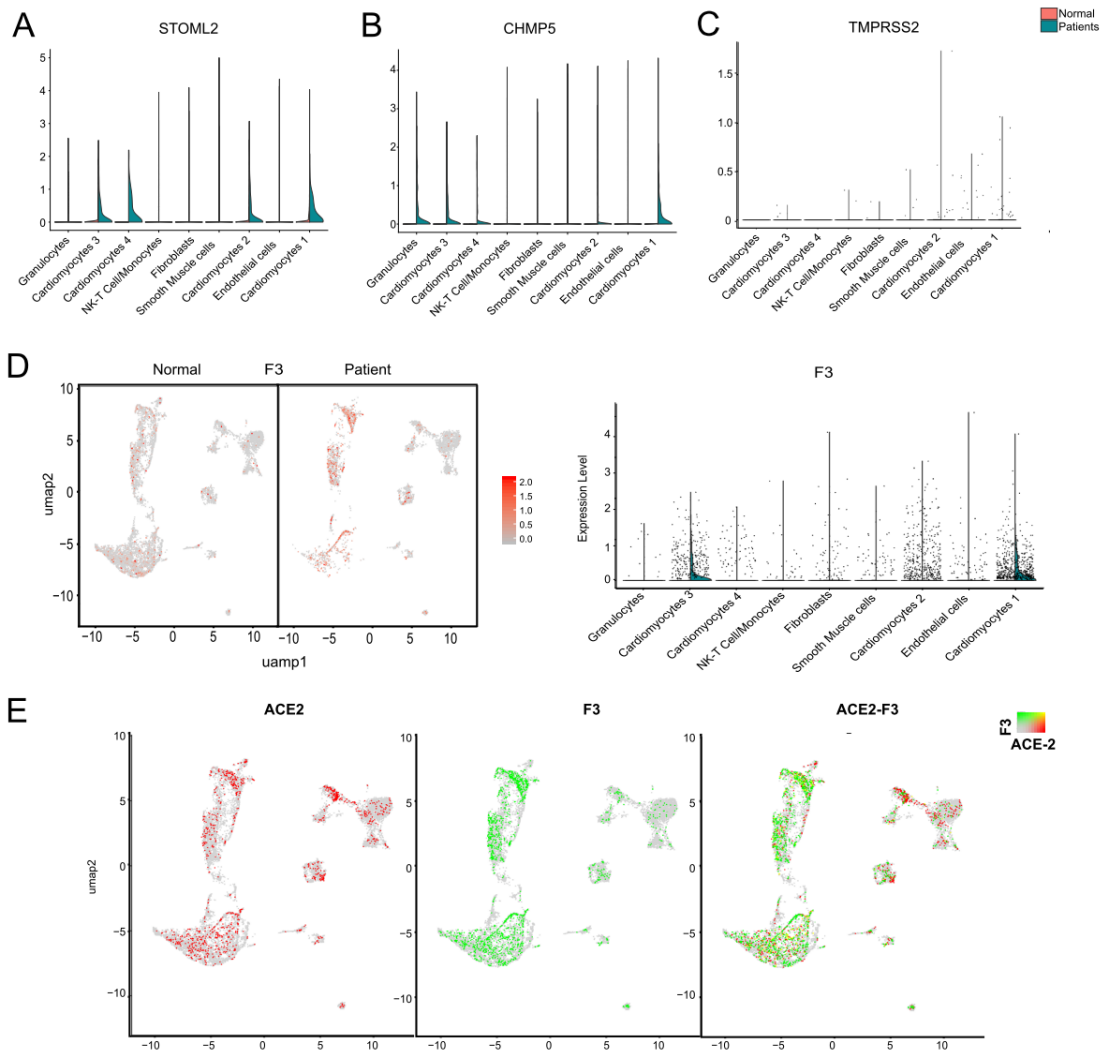

580

581 **Supplemental Figure 2. Distribution of virus-related genes in HF patients compared with**

582 **normal (related to Figure 5)**

583

584 **A,** Violin plots of the distribution of STOML2 related to the biogenesis and activity of

585 mitochondria. **B**, Violin plots of the distribution of CHMP5 related to virus infection. **C**, Violin

586 plots of the distribution of TMPRSS2 related to viral entry. **D**, UMAP of F3 in normal and HF

587 patients (left) and violin plots of the distribution of F3 (right). **E**, Expression level of ACE2

588 (red dots), F3 (green dots) in different subsets, overlapping is shown in the right panel, and the

589 co-expression is shown in yellow dots.

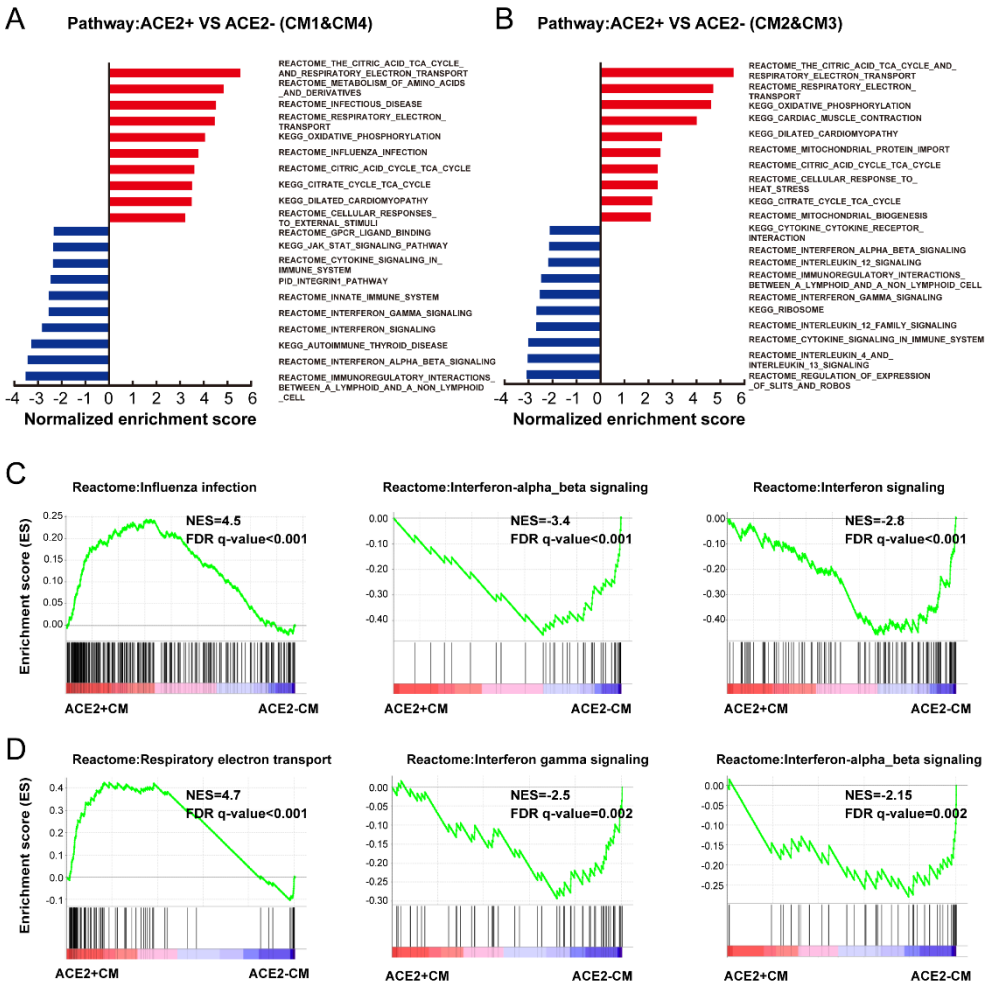

590

591 **Supplemental Figure 3. Characteristics of ACE2 positive ventricular and atrial myocytes**

592 **(related to Figure 6)**

593

594 **A,** Pathway analysis revealed the significant enrichment of biological pathways from

595 comparison of ACE2+ and ACE2- ventricular myocytes. **B**, Pathway analysis revealed the

596 significant enrichment of biological pathways from comparison of ACE2+ and ACE2- atrial

597 myocytes. **C**, Reactome analysis showing the up-regulated influenza infection and down-

598 regulated interferon-alpha_beta signaling and interferon signaling in ventricular myocytes

599 comparison of ACE2+ and ACE2- cells. **D**, Reactome analysis showing the up-regulated

600 respiratory electron transport and down-regulated interferon gamma, interferon-alpha_beta

signaling in atrial myocytes comparison of ACE2+ and ACE2- cells. The NES and false discovery rate (FDR) were showed in panel.

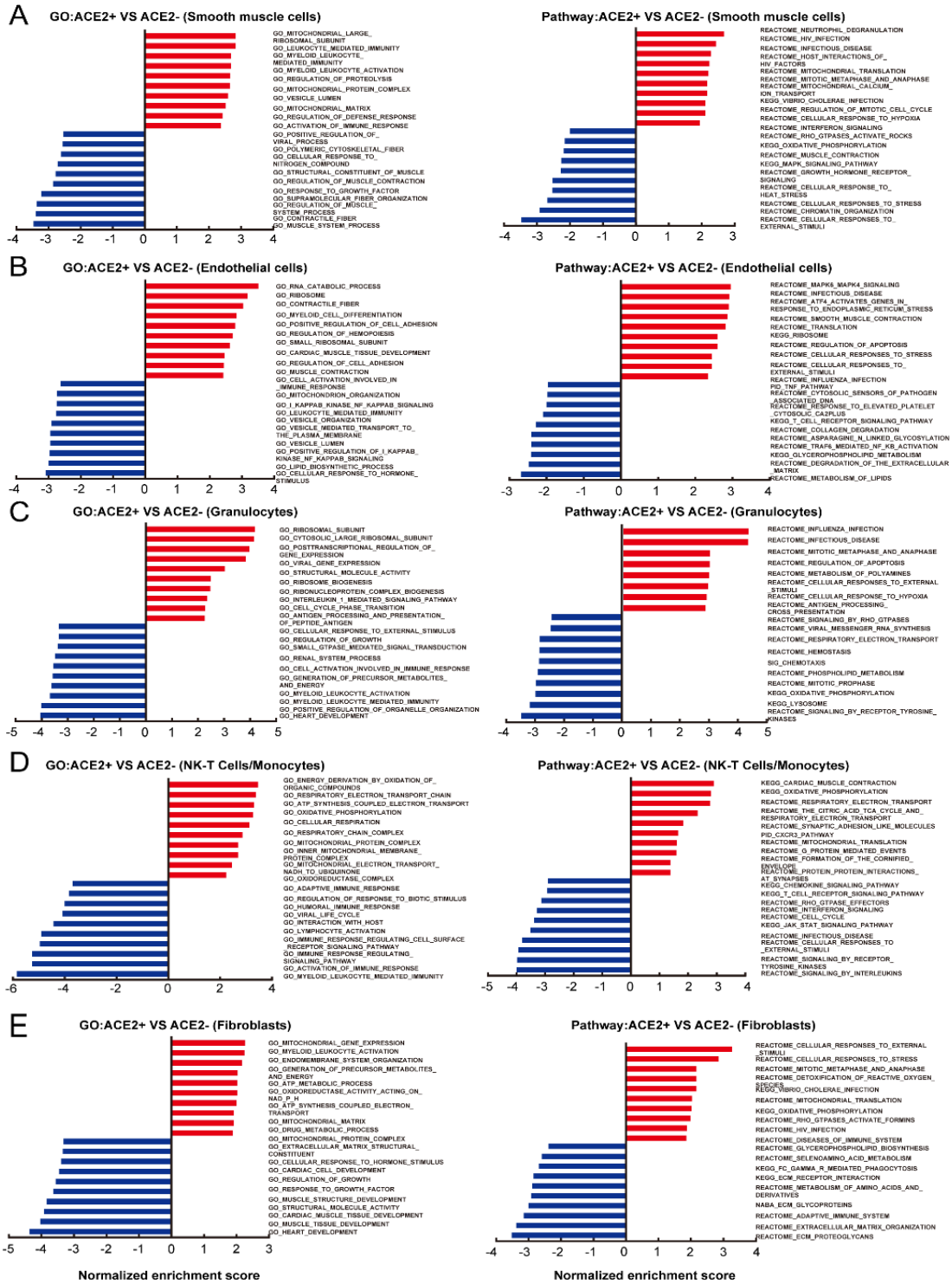

Supplemental Figure 4. Enrichment of biological pathway in different subsets from

606 **comparison of ACE2 positive and negative cells (related to Figure 6)**

607

608 **A-E,** GO and pathway analysis revealed the significant enrichment of biological pathway from

609 comparison of ACE2+ and ACE2- cells in different subsets. **A**, Smooth muscle cells. **B**,

610 endothelial cells. **C**, Granulocytes. **D**, NK-T cells/Monocytes. **E**, Fibroblasts.

611

612